

# VARIATIONAL INFERENCE AIDED ESTIMATION OF TIME VARYING CHANNELS

*Benedikt Böck, Michael Baur, Valentina Rizzello, Wolfgang Utschick*

School of Computation, Information and Technology, Technical University of Munich, Germany  
Email: {benedikt.boeck, mi.baur, valentina.rizzello, utschick}@tum.de

## ABSTRACT

One way to improve the estimation of time varying channels is to incorporate knowledge of previous observations. In this context, Dynamical VAEs (DVAEs) build a promising deep learning (DL) framework which is well suited to learn the distribution of time series data. We introduce a new DVAE architecture, called  $k$ -MemoryMarkovVAE ( $k$ -MMVAE), whose sparsity can be controlled by an additional memory parameter. Following the approach in [1] we derive a  $k$ -MMVAE aided channel estimator which takes temporal correlations of successive observations into account. The results are evaluated on simulated channels by QuaDRiGa and show that the  $k$ -MMVAE aided channel estimator clearly outperforms other machine learning (ML) aided estimators which are either memoryless or naively extended to time varying channels without major adaptations.

**Index Terms**— Time-varying channel estimation, variational inference, deep learning, time series data, MMSE estimator

## 1. INTRODUCTION

Recently, DL aided channel estimation (CE) has demonstrated great performance in a variety of wireless communication systems [1]-[5]. Despite following the general DL paradigm of utilizing data to learn functional dependencies, the core idea of the introduced methods can be divided into two different categories - end-to-end learning and model based learning. In the former the input-output relation of interest is treated as a black box and learned by a neural network while in the latter, isolated parts of a classically modelled relation are replaced by neural networks [6]. Generative models like variational autoencoders (VAEs) and Gaussian mixture models (GMMs) represent promising ML tools which are well suited for model based learning and have shown good results for channel estimation in massive multiple-input multiple-output (MIMO) systems [1, 5]. In these setups, a learnable function maps a channel observation from a fixed environment to the statistical parameters of a so called latent random vector which can be associated with scenario specific characteristics of the corresponding radio propagation environment. The channel can be assumed to be conditionally Gaussian with respect to these characteristics. By utilizing the law of total expectation a parameterized linear minimum mean squared error (LMMSE) estimator can be derived, which is approximately mean squared error (MSE) optimal although the channel can follow any arbitrary distribution. These approaches are solely based on instantaneous channel state information (CSI) and do not take any temporal correlation into account. However, the temporal evolution of the channel is a scenario specific characteristic by itself and further performance gains are expected by incorporating it into a DL aided model for channel estimation.

Our contribution in this work is to extend the VAE framework in [1] to estimate the channel based on correlated channel observations

along a user's trajectory. In this context, we introduce a new DL architecture, called  $k$ -MMVAE, which is motivated by the framework of DVAEs such as KalmanVAEs and Deep Kalman Filters [7, 8]. DVAEs model the latent random vector as a Markov chain and are therefore well suited to represent the temporal correlation in the input data [9]. In contrast to other architectures, our proposed model incorporates an additional memory parameter controlling the sparsity of the corresponding probabilistic graph. Moreover, the VAE aided estimator in [1] as well as the  $k$ -MMVAE are both generalized to take noisy observations with arbitrary signal-to-noise ratios (SNRs) as input. We show that already for very short trajectories the extracted additional information about the temporal evolution leads to significant better estimates compared to the memoryless case. Additionally, we compare our proposed model with a model-agnostic approach, where we process time correlated data from trajectories via an ordinary VAE leading to a noticeable performance decrease.

## 2. SYSTEM AND CHANNEL MODEL

The considered system is a single-input multiple-output (SIMO) setup, in which the base station (BS) is equipped with  $R$  antennas and receives uplink training signals from a single antenna mobile terminal (MT). We concentrate on  $I$  consecutive pilot symbols which are temporally spaced by a time interval  $T$ . After decorrelating the pilots, the resulting received signal  $\mathbf{y}_i$  at time  $iT$  can be expressed as

$$\mathbf{y}_i = \mathbf{h}_i + \mathbf{n}_i \in \mathbb{C}^R, i = 1, \dots, I. \quad (1)$$

The channel vector  $\mathbf{h}_i$  is perturbed by additive white Gaussian noise  $\mathbf{n}_i$  at time  $iT$ , i.e.,  $\mathbf{n}_i \sim \mathcal{N}_{\mathbb{C}}(\mathbf{0}, \sigma_n^2 \mathbf{I})$  and  $\mathbb{E}[\mathbf{n}_i \mathbf{n}_i^H] = \mathbf{0}$  for  $i \neq \tilde{i}$ . We assume the channel vectors of different snapshots to be correlated and the BS antennas to form a uniform linear array (ULA) with half-wavelength spacing. It is known that the resulting channel covariance matrix at any time  $iT$  is Toeplitz structured and can be approximated by a circulant matrix  $\mathbf{C}_i$  for a large number of antennas [10]. Consequently, we can diagonalize  $\mathbf{C}_i$  by utilizing the fact that the eigenvectors of any circulant matrix coincide with the columns of the discrete fourier transform (DFT)-matrix, i.e.,

$$\mathbf{C}_i = \mathbf{F}^H \text{diag}(\mathbf{c}_i) \mathbf{F}, \quad (2)$$

where  $\mathbf{F}$  stands for the  $R \times R$  DFT-matrix.

The channel realizations for training and evaluating the proposed model are generated by the geometry-based stochastic channel modeling tool QuaDRiGa [11, 12]. There, the time dependent channel for a fixed center frequency  $f_c$  is modeled as a superposition of  $L$  distinct propagation paths, i.e.,

$$\mathbf{h}_i = \sum_{l=0}^{L-1} \mathbf{g}_l(iT) \exp(-j2\pi f_c \tau_l(iT)), \quad (3)$$

where  $\tau_l(iT)$  represents the path delay and  $\mathbf{g}_l(iT)$  contains information about path gain, direction of arrival (DoA), polarization effects and subpath characteristics for path  $l$  at time  $iT$ . The initial values of all these parameters are drawn from a scenario specific distribution and are then coherently updated for all snapshots along the user's trajectory. This procedure results in an environment specific time evolution of the channel.

### 3. VARIATIONAL INFERENCE AIDED CHANNEL ESTIMATION

#### 3.1. VAE Preliminaries

Generative models and VAEs in particular aim to learn a distribution  $p(\mathbf{x})$  based on a dataset  $\mathcal{X} = \{\mathbf{x}^{(n)}\}_{n=1}^N$  by applying likelihood estimation to a parameterized statistical model [13]. In order to increase the expressiveness of this model, VAEs introduce a low dimensional non observable (i.e. latent) random vector  $\mathbf{z}$ , such that for each  $\mathbf{x}^{(n)}$  there exists a corresponding realization  $\mathbf{z}^{(n)}$  of  $\mathbf{z}$  which summarizes the key features of  $\mathbf{x}^{(n)}$  [14]. In the standard VAE framework, the distribution of  $\mathbf{z}$ , called prior distribution, is fixed (e.g.  $\mathcal{N}(\mathbf{0}, \mathbf{I})$ ) and the conditional distribution  $p_\theta(\mathbf{x}|\mathbf{z})$  is parameterized by a learnable parameter  $\theta$  representing e.g. the weights of a neural network. A drawback of introducing  $\mathbf{z}$  is that the resulting marginalized likelihood  $p_\theta(\mathbf{x})$  is not computable due to the intractability of  $p_\theta(\mathbf{z}|\mathbf{x})$ . To overcome this issue,  $p_\theta(\mathbf{z}|\mathbf{x})$  is approximately inferred by minimizing the Kullback-Leibler (KL) divergence between  $p_\theta(\mathbf{z}|\mathbf{x})$  and a tractable distribution  $q_\phi(\mathbf{z}|\mathbf{x})$ . The parameter  $\phi$  is learnable and stands for e.g. the weights of a neural network. By subtracting this KL divergence from the log likelihood, the resulting expression is a tractable lower bound on the log likelihood  $\log p_\theta(\mathbf{x})$  called evidence-lower bound (ELBO)  $\mathcal{L}(\theta, \phi)$ . Assuming that the samples in  $\mathcal{X}$  are independent and identically distributed (i.i.d.), an equivalent and more practical version of the ELBO is given by

$$\mathcal{L}(\theta, \phi) = \sum_{n=1}^N \mathbb{E}_{q_\phi(\mathbf{z}|\mathbf{x}^{(n)})} \left[ \log p_\theta(\mathbf{x}^{(n)}|\mathbf{z}) - \log \frac{q_\phi(\mathbf{z}|\mathbf{x}^{(n)})}{p(\mathbf{z})} \right]. \quad (4)$$

Usually, the expectation is approximated by a Monte-Carlo estimation based on a single sample drawn from  $q_\phi(\mathbf{z}|\mathbf{x}^{(n)})$ . The relation between  $\mathbf{x}$  and  $\mathbf{z}$  is represented as probabilistic graph in Fig. 1 a), in which the parameterized statistical model  $p_\theta(\mathbf{x}|\mathbf{z})$  is illustrated by the solid arrow and can be distinguished from the approximate inference distribution  $q_\phi(\mathbf{z}|\mathbf{x})$  displayed as a dashed arrow. In standard VAEs,  $q_\phi(\mathbf{z}|\mathbf{x})$ , as well as  $p_\theta(\mathbf{x}|\mathbf{z})$ , are modeled as conditionally Gaussian distributions with means  $\boldsymbol{\mu}_\theta(\mathbf{z})$  and  $\boldsymbol{\mu}_\phi(\mathbf{x})$ , and diagonal covariance matrices  $\text{diag}(\boldsymbol{\sigma}_\theta(\mathbf{z})^2)$  and  $\text{diag}(\boldsymbol{\sigma}_\phi(\mathbf{x})^2)$ , respectively.

The corresponding architecture is illustrated in Fig. 1 b). The parameterization  $\phi$  is realized by a neural network, called encoder, which takes a sample  $\mathbf{x}$  as input and outputs  $\boldsymbol{\mu}_\phi(\mathbf{x})$ , as well as  $\boldsymbol{\sigma}_\phi(\mathbf{x})$ . Subsequently, a single sample  $\tilde{\mathbf{z}}$  is drawn from  $q_\phi(\mathbf{z}|\mathbf{x})$  by computing it via  $\tilde{\mathbf{z}} = \boldsymbol{\mu}_\phi(\mathbf{x}) + \boldsymbol{\sigma}_\phi(\mathbf{x}) \odot \boldsymbol{\epsilon}$  where  $\boldsymbol{\epsilon} \sim \mathcal{N}(\mathbf{0}, \mathbf{I})$ . This is known as the reparameterization trick. Eventually, a second neural network, called decoder, takes  $\tilde{\mathbf{z}}$  as input and outputs  $\boldsymbol{\mu}_\theta(\tilde{\mathbf{z}})$  as well as  $\boldsymbol{\sigma}_\theta(\tilde{\mathbf{z}})$ . Based on these parameters, the ELBO can be evaluated and maximized by a gradient based optimization algorithm.

#### 3.2. VAE Based CE with Instantaneous CSI

There are several ways how to utilize standard VAEs for channel estimation based on instantaneous CSI. In this section, we give a brief

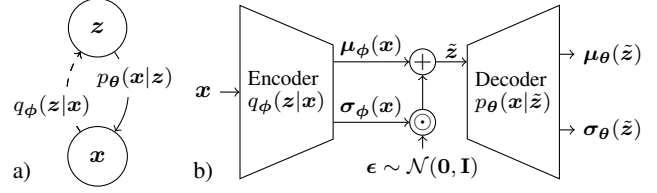


**Fig. 1:** Probabilistic graph (a) and architecture (b) of the standard VAE framework.

overview of the key concepts by focusing on one particular way and refer to [1] for a more detailed explanation. The data set  $\mathcal{X}$  consists of i.i.d. channel realizations  $\{\mathbf{h}^{(n)}\}_{n=1}^N$  at single time instances. In this case, the approximate inference distribution  $q_\phi(\mathbf{z}|\cdot)$  is conditioned on noisy observations  $\mathbf{y}$  of the samples in  $\mathcal{X}$  according to (1). Consequently, perfect CSI in form of noiseless channel realizations is only required during the training phase. The law of total expectation

$$\mathbb{E}_{p(\mathbf{h}|\mathbf{y})}[\mathbf{h}|\mathbf{y}] = \mathbb{E}_{p(\mathbf{z}|\mathbf{y})}[\mathbb{E}_{p(\mathbf{h}|\mathbf{y},\mathbf{z})}[\mathbf{h}|\mathbf{y},\mathbf{z}]] \quad (5)$$

is used to reformulate the minimum mean squared error (MMSE) estimator as an expected LMMSE estimator

$$\mathbb{E}_{p(\mathbf{z}|\mathbf{y})}[\boldsymbol{\mu}_{\mathbf{h}|\mathbf{z}} + \mathbf{C}_{\mathbf{h}|\mathbf{z}}(\mathbf{C}_{\mathbf{h}|\mathbf{z}} + \sigma_n^2 \mathbf{I})^{-1}(\mathbf{y} - \boldsymbol{\mu}_{\mathbf{h}|\mathbf{z}})]. \quad (6)$$

The parameters  $\boldsymbol{\mu}_{\mathbf{h}|\mathbf{z}}$  and  $\mathbf{C}_{\mathbf{h}|\mathbf{z}}$  are mean and covariance matrix of the channel  $\mathbf{h}$  conditioned on the latent random vector  $\mathbf{z}$ . As explained in Section 2,  $\mathbf{C}_{\mathbf{h}|\mathbf{z}}$  can be assumed to be diagonal by preprocessing the noiseless as well as the noisy channel realizations by a DFT transformation. The estimator in (6) can therefore be approximated by an ML aided LMMSE estimator for which the expectation operation can be dropped by replacing  $\boldsymbol{\mu}_{\mathbf{h}|\mathbf{z}}$  and  $\mathbf{C}_{\mathbf{h}|\mathbf{z}}$  with the VAE learned parameters  $\boldsymbol{\mu}_\theta(\boldsymbol{\mu}_\phi(\mathbf{y}))$  and  $\text{diag}(\boldsymbol{\sigma}_\theta(\boldsymbol{\mu}_\phi(\mathbf{y}))^2)$ .

#### 3.3. Dynamical VAE Preliminaries

The standard VAE enforces the entries of  $\mathbf{z}$  as well as  $\mathbf{x}|\mathbf{z}$  to be mutually independent by modeling the corresponding covariance matrices to be diagonal. However, there are applications for which this assumption does not reflect the actual structure of the given data. One example are stochastic processes, where a single sample  $\mathbf{x}$  consists of  $I$  successively sampled and potentially correlated values  $\mathbf{x}_i$ , i.e.,  $\mathbf{x} = [\mathbf{x}_1^T, \dots, \mathbf{x}_I^T]^T$ . DVAEs form an extended VAE framework and consider temporal correlations within a single sample  $\mathbf{x}$  by introducing dependencies between entries of the latent random vector  $\mathbf{z}$  [9]. A common choice is to model  $\mathbf{z}$  as a Markov chain with parameterized transition probabilities, i.e.,

$$p_\gamma(\mathbf{z}) = \prod_{i=1}^I p_{\gamma_i}(\mathbf{z}_i|\mathbf{z}_{i-1}), \quad (7)$$

where  $\mathbf{z} = [\mathbf{z}_1^T, \dots, \mathbf{z}_I^T]^T$  and  $\mathbf{z}_0 = \emptyset$ . The parameter  $\gamma = [\gamma_1^T, \dots, \gamma_I^T]^T$  is learnable and can be implemented in different ways. One example is the KalmanVAE, in which  $\gamma_i$  parameterizes a linear state space model [7]. In contrast, Deep Kalman Filters realize  $\gamma_i$  by a neural network which outputs the mean and covariance matrix of  $\mathbf{z}_i|\mathbf{z}_{i-1}$  [8]. Besides the distribution of  $\mathbf{z}$ ,  $q_\phi(\mathbf{z}|\mathbf{x})$  and  $p_\theta(\mathbf{z}|\mathbf{x})$  are also tailored to the given data structure and can be decomposed similarly to  $p_\gamma(\mathbf{z})$  in (7). By modeling the latent space as a Markov chain according to (7),  $\mathbf{z}_i$  depends on the realization of  $\mathbf{z}_{i-1}$  which is commonly incorporated in the decomposition of

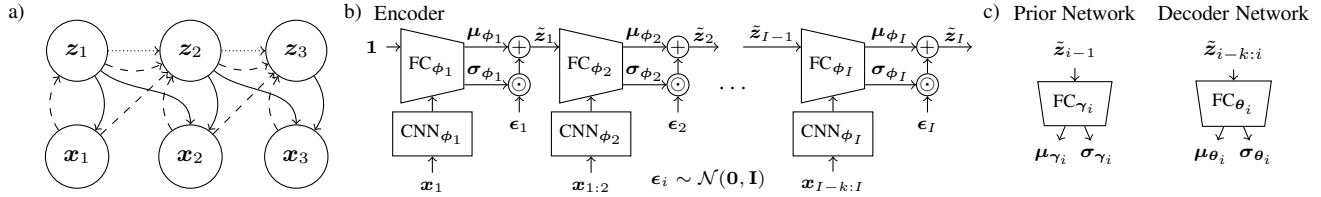


**Fig. 2:** Probabilistic graph (a), encoder architecture (b), and decoder and prior network architecture (c) of the  $k$ -MMVAE.

$q_\phi(\mathbf{z}|\mathbf{x})$ . Additionally, the ELBO is adapted and an iterative sampling procedure is introduced keeping the computation of the ELBO efficient. This is explained in more detail in Section 3.4 based on our proposed model.

### 3.4. $k$ -MemoryMarkovVAE

In this work, we propose an adapted DVAE architecture, called  $k$ -MemoryMarkovVAE, which to the best of our knowledge, has not been introduced in other publications. Just like KalmanVAEs and Deep Kalman Filters,  $k$ -MMVAEs model the latent space as a Markov chain according to (7). In contrast to other DVAEs however, we introduce an adjustable hyperparameter  $k$  standing for the memory of  $q_\phi(\mathbf{z}|\mathbf{x})$  and  $p_\theta(\mathbf{z}|\mathbf{x})$ . More precisely, these distributions are decomposed as

$$q_\phi(\mathbf{z}|\mathbf{x}) = \prod_i q_{\phi_i}(\mathbf{z}_i|\mathbf{z}_{i-1}, \mathbf{x}_{i-k:i}) \quad (8)$$

$$p_\theta(\mathbf{x}|\mathbf{z}) = \prod_i p_{\theta_i}(\mathbf{x}_i|\mathbf{z}_{i-k:i}) \quad (9)$$

with  $\mathbf{x}_{i-k:i} = [\mathbf{x}_{i-k}^T, \dots, \mathbf{x}_i^T]^T$ ,  $\mathbf{z}_{i-k:i} = [\mathbf{z}_{i-k}^T, \dots, \mathbf{z}_i^T]^T$ . The memory  $k$  represents a trade-off between the expressiveness of the model and the extent to which the model is tailored to a particular task. In Fig. 2 a) the corresponding probabilistic graph for  $I = 3$  and  $k = 1$  is shown. The dotted, dashed and solid arrows stand for the dependencies in  $p_\gamma(\mathbf{z})$ ,  $q_\phi(\mathbf{z}|\mathbf{x})$ , and  $p_\theta(\mathbf{x}|\mathbf{z})$ , respectively. If  $k$  is set to 0, the independence assumptions equal those of a Kalman Filter and result in a highly sparse probabilistic graph. However, by increasing the parameter  $k$ , further dependencies are added and the sparsity level decreases. Since information about the distribution and temporal evolution of some scenario specific characteristics like doppler shifts can only be extracted from a sequence of channel observations, keeping the possibility of a nonzero  $k$  is reasonable in the context of estimating wireless channels. By inserting (7), (8) and (9) into the definition of the ELBO in (4), the new objective can be stated as

$$\mathcal{L}^{(D)} = \sum_{n,i=1}^{N,I} \mathbb{E}_{q_{\phi_{1:i}}} \left[ \log \frac{p_{\theta_i}(\mathbf{x}_i^{(n)}|\mathbf{z}_{i-k:i})p_{\gamma_i}(\mathbf{z}_i|\mathbf{z}_{i-1})}{q_{\phi_i}(\mathbf{z}_i|\mathbf{z}_{i-1}, \mathbf{x}_{i-k:i})} \right], \quad (10)$$

where  $q_{\phi_{1:i}} = \prod_{i'=1}^i q_{\phi_{i'}}(\mathbf{z}_{i'}|\mathbf{z}_{i'-1}, \mathbf{x}_{i'-k:i'})$ . Similiary to standard VAEs, the parameterized distributions  $p_{\gamma_i}(\mathbf{z}_i|\mathbf{z}_{i-1})$ ,  $q_{\phi_i}(\mathbf{z}_i|\mathbf{z}_{i-1}, \mathbf{x}_{i-k:i})$  and  $p_{\theta_i}(\mathbf{x}_i|\mathbf{z}_{i-k:i})$  are modeled as Gaussians with means  $\boldsymbol{\mu}_{\gamma_i}(\mathbf{z}_{i-1})$ ,  $\boldsymbol{\mu}_{\phi_i}(\mathbf{z}_{i-1}, \mathbf{x}_{i-k:i})$  and  $\boldsymbol{\mu}_{\theta_i}(\mathbf{z}_{i-k:i})$ , and covariance matrices  $\text{diag}(\boldsymbol{\sigma}_{\gamma_i}(\mathbf{z}_{i-1})^2)$ ,  $\text{diag}(\boldsymbol{\sigma}_{\phi_i}(\mathbf{z}_{i-1}, \mathbf{x}_{i-k:i})^2)$  and  $\text{diag}(\boldsymbol{\sigma}_{\theta_i}(\mathbf{z}_{i-k:i})^2)$ , respectively. Additionally, the expectation operations in (10) are approximated by single sample Monte-Carlo estimations embedded in the encoder architecture. This is illustrated in Fig. 2 b). The encoder is realized by  $I$  ordered neural networks, where each one concatenates a convolutional neural network (CNN)

with a fully connected (FC) neural network and is followed by a sampling operation. The first encoder network outputs the mean  $\boldsymbol{\mu}_{\phi_1}(\mathbf{x}_1)$  and variances  $\boldsymbol{\sigma}_{\phi_1}(\mathbf{x}_1)$  of  $q_{\phi_1}(\mathbf{z}_1|\mathbf{x}_1)$  from which a sample  $\tilde{\mathbf{z}}_1$  is drawn from. This in turn is fed to the second encoder network computing  $\boldsymbol{\mu}_{\phi_2}(\tilde{\mathbf{z}}_1, \mathbf{x}_{1:2})$  and  $\boldsymbol{\sigma}_{\phi_2}(\tilde{\mathbf{z}}_1, \mathbf{x}_{1:2})$  such that a further sample  $\tilde{\mathbf{z}}_2$  can be drawn from  $q_{\phi_2}(\mathbf{z}_2|\tilde{\mathbf{z}}_1, \mathbf{x}_{1:2})$ . By repeating this procedure for all  $I$  states we end up with a sample  $\tilde{\mathbf{z}}$  drawn from  $q_\phi(\mathbf{z}|\mathbf{x})$  in (8). In this way, we can maximize the ELBO  $\mathcal{L}^{(D)}$  by a gradient based optimization algorithm over  $\boldsymbol{\theta}$ ,  $\boldsymbol{\phi}$  and  $\boldsymbol{\gamma}$ . The parameters  $\boldsymbol{\theta}$  and  $\boldsymbol{\gamma}$  are also implemented by  $I$  distinct neural networks illustrated in Fig. 2 c). A FC neural network, called prior network, takes  $\tilde{\mathbf{z}}_{i-1}$  as input, and outputs  $\boldsymbol{\mu}_{\gamma_i}(\tilde{\mathbf{z}}_{i-1})$  and  $\boldsymbol{\sigma}_{\gamma_i}(\tilde{\mathbf{z}}_{i-1})$ . On the other hand, another FC neural network, called decoder network, outputs  $\boldsymbol{\mu}_{\theta_i}(\tilde{\mathbf{z}}_{i-k:i})$  and  $\boldsymbol{\sigma}_{\theta_i}(\tilde{\mathbf{z}}_{i-k:i})$  based on the input  $\tilde{\mathbf{z}}_{i-k:i}$ . The parameters  $\log \boldsymbol{\sigma}_{\gamma_i}$  and  $\log \boldsymbol{\sigma}_{\phi_i}$  are additionally bounded to improve the stability during training. In contrast to ordinary recurrent neural networks, no parameter sharing is utilized and there exist separate networks for each state  $i$ . The memory  $k$ , the latent dimension of  $\mathbf{z}_i$ , the widths and depths of the neural networks and the kernel size of the CNN are determined via a network architecture search. The model leading to the largest ELBO computed on an evaluation set is chosen.

The  $k$ -MMVAE can be utilized in a similar way as the standard VAE for ML aided channel estimation. The dataset  $\mathcal{X}$  consists of  $I$  consecutive channel realizations along  $N$  trajectories and the distributions  $q_{\phi_i}(\mathbf{z}_i|\mathbf{z}_{i-1}, \cdot)$  are conditioned on noisy observations  $\mathbf{y}_{i-k:i}$  of the channel realizations according to (1). An estimation of the  $i$ -th channel realization  $\mathbf{h}_i$  is obtained as follows. The first encoder network computes  $\boldsymbol{\mu}_{\phi_1}(\mathbf{y}_1)$  and forwards it to the next encoder network computing  $\boldsymbol{\mu}_{\phi_2}(\boldsymbol{\mu}_{\phi_1}, \mathbf{y}_{1:2})$ . This in turn is used as input for the subsequent encoder network and is repeated up to the  $i$ -th time instance resulting in a sequence of means  $\boldsymbol{\mu}_{\phi_{1:i}} = [\boldsymbol{\mu}_{\phi_1}^T, \dots, \boldsymbol{\mu}_{\phi_i}^T]^T$ . Eventually, the  $i$ -th decoder network can compute  $\boldsymbol{\mu}_{\theta_i}(\boldsymbol{\mu}_{\phi_{i-k:i}})$  and  $\text{diag}(\boldsymbol{\sigma}_{\theta_i}(\boldsymbol{\mu}_{\phi_{i-k:i}})^2)$ . Based on these outputs, an approximated MMSE channel estimator is obtained from (6), where the expectation operation is dropped by replacing  $\boldsymbol{\mu}_{\mathbf{h}|\mathbf{z}}$  and  $\mathbf{C}_{\mathbf{h}|\mathbf{z}}$  with  $\boldsymbol{\mu}_{\theta_i}(\boldsymbol{\mu}_{\phi_{i-k:i}})$  and  $\text{diag}(\boldsymbol{\sigma}_{\theta_i}(\boldsymbol{\mu}_{\phi_{i-k:i}})^2)$ , respectively.

### 3.5. Related Channel Estimators

We compare our proposed model to several other estimators. All methods are evaluated with respect to estimating the channel  $\mathbf{h}_{\tilde{i}}$  of one fixed time instance  $\tilde{i}$ . As baseline for those which do not utilize ML, we take the least squares (LS) estimator  $\hat{\mathbf{h}}_{\tilde{i}}^{(LS)} = \mathbf{y}_{\tilde{i}}$  and an LMMSE estimator  $\hat{\mathbf{h}}_{\tilde{i}}^{(sCov)}$  based on the sample covariance matrix  $\hat{\mathbf{C}}_{\tilde{i}} = (1/N) \sum_{n=1}^N (\mathbf{h}_{\tilde{i}}^{(n)} - \bar{\mathbf{h}}_{\tilde{i}}^{(n)})(\mathbf{h}_{\tilde{i}}^{(n)} - \bar{\mathbf{h}}_{\tilde{i}}^{(n)})^H$  with  $\bar{\mathbf{h}}_{\tilde{i}}^{(n)}$  being the sample mean. The dataset  $\mathcal{X}_{\tilde{i}}$  used in this case contains the channel realizations of the particular time instance  $\tilde{i}$  along all trajectories in  $\mathcal{X}$ , for which the channel estimation is evaluated. Additionally, we compare our model with the VAE based estimator from [1], which is

explained in Section 3.2 and for which the dataset  $\mathcal{X}_i$  is utilized as well. All these estimators solely rely on instantaneous CSI. Therefore, we also consider a standard VAE, called TSVAE, which takes a noisy observation of the whole trajectory as input and outputs the statistical characteristics of the channel at the time instance  $i$ , which can be used to estimate  $\mathbf{h}_i$  in the same manner as it is described in Section 3.2.

#### 4. SIMULATION RESULTS

The generated trajectories in QuaDRiGa are simulated in a 3GPP 38.901 urban macro cell with mixed NLOS/LOS channels and 80% indoor users. The number of snapshots per trajectory is set to 8 and the velocity for each user is drawn from a Rayleigh distribution with parameter  $\sigma^2 = 4$ . Motivated by the 5G standards, the center frequency is set to 2.1 GHz and the time interval  $T$  between two successive snapshots is set to 0.5 ms. The number of antennas  $R$  at the BS is 32. The data set is split into training, evaluation and test set with 100000, 10000 and 10000 trajectories, respectively. The channels along each trajectory are preprocessed separately by removing the average path gain over the snapshots as described in the QuaDRiGa documentation [12]. Moreover, the channels are normalized such that the average channel power of the 8-th snapshot  $(1/N) \sum_{n=1}^N \|\mathbf{h}_8^{(n)}\|_2^2$  equals the number of BS antennas. The noise variance is determined at a particular SNR for each trajectory individually by  $\sigma_n^{(n)2} = \|\mathbf{h}_8^{(n)}\|_2^2 / (R \cdot \text{SNR})$ . New noisy observations  $\mathbf{y}_i^{(n)}$  are generated for each epoch during the training. This is done by first drawing a value for the SNR in dB from a uniform distribution between -10 dB and 25 dB and then drawing a noise vector from  $\mathcal{N}_C(\mathbf{0}, \sigma_n^{(n)2} \mathbf{I})$  for every snapshot along the trajectory. An adaptive learning rate is used which is initialized with  $6 \cdot 10^{-5}$  and once divided by a factor of 5 when the ELBO remains constant within 25 epochs on the evaluation set. The ELBO in (10) is taken as objective which is additionally regularized by the method of free bits and maximized by the Adam optimizer [13, 15].

The channel estimators are evaluated based on a snapshot-wise normalized mean squared error (NMSE) defined as

$$\text{NMSE}_i = \frac{1}{N_t} \sum_{n=1}^{N_t} \frac{\|\mathbf{h}_i^{(n)} - \hat{\mathbf{h}}_i^{(n)}\|_2^2}{\|\mathbf{h}_i^{(n)}\|_2^2}, \quad (11)$$

where  $N_t$  is the number of samples in the test set and  $\hat{\mathbf{h}}_i^{(n)}$  is the estimate of  $\mathbf{h}_i^{(n)}$ . Fig. 3 shows the performance for an SNR range between -5 and 20 dB, where all methods are evaluated on the channel realizations of the 8-th snapshot. The data set  $\mathcal{X}_8$  defined in Section 3.5 is used for the estimators considering solely instantaneous CSI. The  $k$ -MMVAE aided estimator clearly outperforms the other models for all SNR values. The model agnostic standard VAE which takes the entire trajectory as input, called TSVAE, only performs slightly better than the standard VAE considering only instantaneous CSI. A reasonable explanation is that the TSVAE maps the trajectory on a standard normal distributed latent random vector  $\mathbf{z}$  which cannot comprise temporal correlations efficiently. The LS as well as the sample covariance estimator are generally worse than the ML aided ones. This is expected since the sample covariance estimator is MSE suboptimal for non-Gaussian distributed channels which usually holds. The LS estimator does not incorporate any scenario specific information at all. The  $k$ -MMVAE also provides the possibility to estimate all channels  $\mathbf{h}_i$  along the trajectory which is shown in Fig. 4. The  $k$ -MMVAE as well as the VAE aided estimator are evaluated on every snapshot of the trajectory with a fixed SNR of

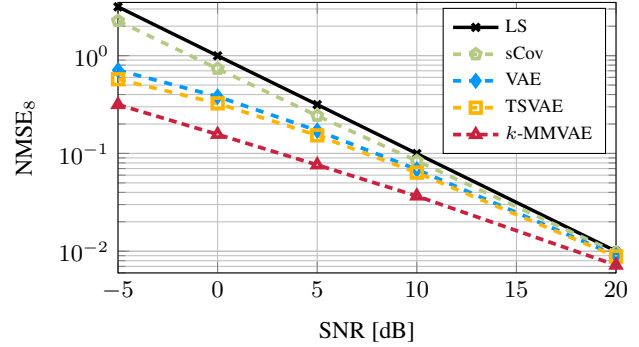


Fig. 3: NMSE<sub>8</sub> over SNR of the different estimators. The  $k$ -MMVAE aided estimator is displayed in red.

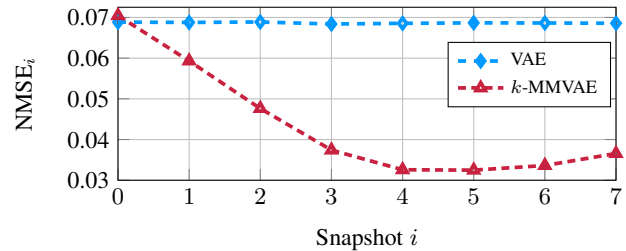


Fig. 4: NMSE over snapshots for 10 dB SNR. The memoryless VAE aided estimator is displayed in blue. The  $k$ -MMVAE aided one is shown in red.

10 dB. Since the latter only considers instantaneous CSI it performs the same in all cases. It can be seen how the  $k$ -MMVAE utilizes the knowledge of previous observations and improves the performance successively over the snapshots. For the last few time instances however, the NMSE remains static and increases slightly. A possible explanation for this behaviour is, that the iterative sampling procedure explained in Section 3.4 leads to different importance levels of the learned parameters. More precisely, since the  $i$ -th drawn sample from  $q_{\phi_i}(\mathbf{z}_i | \tilde{\mathbf{z}}_{i-1}, \mathbf{x}_{i-k:i}^{(n)})$  depends on the parameters  $\phi_{1:i-1}$ , the encoder networks of the first few snapshots have more impact on which optimum is reached and are therefore adjusted more carefully than the encoder networks of the last snapshots.

The results indicate that ML aided channel estimation can be improved significantly by incorporating the temporal evolution of the channel into the architecture. This, however, cannot be done in a straightforward and model agnostic fashion as it is done for the TSVAE estimator. Instead, a tailored method like the  $k$ -MMVAE aided estimator in which temporal characteristics can be learned efficiently, is beneficial.

#### 5. CONCLUSION

In this work, we introduced a new DVAE architecture, called  $k$ -MMVAE and used it to extend the ML aided channel estimator in [1] to temporally correlated channels along trajectories. Our simulations showed that the model leads to notably better estimates compared to other ML aided estimators. However, other applications like channel prediction for which the  $k$ -MMVAE could be considered have not yet been investigated. This topic together with a more detailed comparison to other DVAE architectures and further classical estimators will be addressed in future work.

## 6. REFERENCES

- [1] M. Baur, B. Fesl, K. Michael, and W. Utschick, "Variational Autoencoder Leveraged MMSE Channel Estimation," *56th Asilomar Conference on Signals, Systems, and Computers*, 2022, accepted for publication.
- [2] M. Soltani, V. Pourahmadi, A. Mirzaei, and H. Sheikhzadeh, "Deep Learning-Based Channel Estimation," *IEEE Communications Letters*, vol. 23, no. 4, pp. 652–655, 2019.
- [3] H. Ye, G. Y. Li, and B. Juang, "Power of Deep Learning for Channel Estimation and Signal Detection in OFDM Systems," *IEEE Wireless Communications Letters*, vol. 7, no. 1, pp. 114–117, 2018.
- [4] D. Neumann, T. Wiese, and W. Utschick, "Learning the MMSE Channel Estimator," *IEEE Transactions on Signal Processing*, vol. 66, no. 11, pp. 2905–2917, 2018.
- [5] M. Koller, B. Fesl, N. Turan, and W. Utschick, "An Asymptotically MSE-Optimal Estimator Based on Gaussian Mixture Models," *IEEE Transactions on Signal Processing*, vol. 70, pp. 4109–4123, 2022.
- [6] N. Shlezinger, J. Whang, Y. C. Eldar, and A. G. Dimakis, "Model-Based Deep Learning: Key Approaches and Design Guidelines," in *2021 IEEE Data Science and Learning Workshop (DSLW)*, 2021, pp. 1–6.
- [7] M. Fraccaro, S. Kamronn, U. Paquet, and O. Winther, "A Disentangled Recognition and Nonlinear Dynamics Model for Unsupervised Learning," in *Advances in Neural Information Processing Systems*. 2017, vol. 30, Curran Associates, Inc.
- [8] R. G. Krishnan, U. Shalit, and D. A. Sontag, "Deep Kalman Filters," *CoRR*, vol. abs/1511.05121, 2015.
- [9] L. Girin, S. Leglaive, X. Bie, J. Diard, T. Hueber, and X. Alameda-Pineda, "Dynamical Variational Autoencoders: A Comprehensive Review," *Found. Trends Mach. Learn.*, vol. 15, no. 1-2, pp. 1–175, 2021.
- [10] R. M. Gray, "Toeplitz and Circulant Matrices: A Review," *Found. and Trends® in Commun. and Inf. Theory*, , no. 3, pp. 155 – 239, 2006.
- [11] S. Jaeckel, L. Raschkowski, K. Boerner, and L. Thiele, "QuaDRiGa: A 3-D Multi-Cell Channel Model With Time Evolution for Enabling Virtual Field Trials," *IEEE Transactions on Antennas and Propagation*, vol. 62, no. 6, pp. 3242–3256, 2014.
- [12] S. Jaeckel, L. Raschkowski, K. Boerner, F. Burkhardt, L. Thiele, and E. Eberlein, "QuaDRiGa - Quasi Deterministic Radio Channel Generator, User Manual and Documentation," 2021, Tech. Rep. v2.6.1.
- [13] D. P. Kingma and M. Welling, "An Introduction to Variational Autoencoders," *Found. Trends Mach. Learn.*, vol. 12, no. 4, pp. 307–392, 2019.
- [14] D. P. Kingma and M. Welling, "Auto-Encoding Variational Bayes," in *2nd International Conference on Learning Representations*, 2014.
- [15] D. P. Kingma and J. Ba, "Adam: A Method for Stochastic Optimization," in *3rd International Conference on Learning Representations 2015*, 2015.